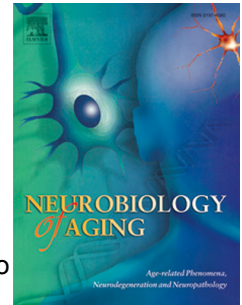


Accepted Manuscript

Abnormal Trajectories in Cerebellum and Brainstem Volumes in Carriers of the Fragile X Premutation

Jun Yi Wang, David Hessel, Randi J. Hagerman, Tony J. Simon, Flora Tassone, Emilio Ferrer, Susan M. Rivera



PII: S0197-4580(17)30092-1

DOI: [10.1016/j.neurobiolaging.2017.03.018](https://doi.org/10.1016/j.neurobiolaging.2017.03.018)

Reference: NBA 9877

To appear in: *Neurobiology of Aging*

Received Date: 24 August 2016

Revised Date: 27 January 2017

Accepted Date: 10 March 2017

Please cite this article as: Wang, J.Y., Hessel, D., Hagerman, R.J., Simon, T.J., Tassone, F., Ferrer, E., Rivera, S.M., Abnormal Trajectories in Cerebellum and Brainstem Volumes in Carriers of the Fragile X Premutation, *Neurobiology of Aging* (2017), doi: 10.1016/j.neurobiolaging.2017.03.018.

This is a PDF file of an unedited manuscript that has been accepted for publication. As a service to our customers we are providing this early version of the manuscript. The manuscript will undergo copyediting, typesetting, and review of the resulting proof before it is published in its final form. Please note that during the production process errors may be discovered which could affect the content, and all legal disclaimers that apply to the journal pertain.

Abnormal Trajectories in Cerebellum and Brainstem Volumes in Carriers of the Fragile X Premutation

Jun Yi Wang,^a David Hessel,^{b,c} Randi J. Hagerman,^{b,d} Tony J. Simon,^{b,c} Flora Tassone,^{b,e} Emilio Ferrer^f and Susan M. Rivera^{a,b,f}

^a Center for Mind and Brain, University of California-Davis, Davis, CA, USA

^b Medical Investigation of Neurodevelopmental Disorders (MIND) Institute, University of California-Davis Medical Center, Sacramento, CA, USA

^c Department of Psychiatry and Behavioral Sciences, University of California-Davis, School of Medicine, Sacramento, CA, USA

^d Department of Pediatrics, University of California-Davis, School of Medicine, Sacramento, CA, USA

^e Department of Biochemistry and Molecular Medicine, University of California-Davis, School of Medicine, Sacramento, CA, USA

^f Department of Psychology, University of California-Davis, Davis, CA, USA

Correspondence: Dr. Jun Yi Wang

Address: Center for Mind and Brain, 267 Cousteau Place, Davis, CA 95618

Phone: 530.747.3802, *Fax:* 530.297.4603

Email: jiwang@ucdavis.edu

Abstract

Fragile X-associated tremor/ataxia syndrome (FXTAS) is a late-onset neurodegenerative disorder typically affecting male premutation carriers with 55-200 CGG repeat expansions in the *FMR1* gene after age 50. The aim of this study was to examine whether cerebellar and brainstem changes emerge during development or aging in late life. We retrospectively analyzed MRI scans from 322 males (age 8-81 years). Volume changes in the cerebellum and brainstem were contrasted with those in the ventricles and whole brain. Compared to the controls, premutation carriers without FXTAS showed significantly accelerated volume decrease in the cerebellum and whole brain, flatter inverted U-shaped trajectory of the brainstem, and larger ventricles. Compared to both older controls and premutation carriers without FXTAS, carriers with FXTAS exhibited significant volume decrease in the cerebellum and whole brain and accelerated volume decrease in the brainstem. We therefore conclude that cerebellar and brainstem volumes were likely affected during both development and progression of neurodegeneration in premutation carriers, suggesting that interventions may need to start early in adulthood to be most effective.

Keywords: fragile X; FXTAS; fragile X premutation; *FMR1*; MRI; neurodegenerative disorder

Abbreviations: CSP, cavum septum pellucidum; CV, cavum vergae; FMRP, fragile X mental retardation protein; FXPOI, fragile X-associated primary ovarian insufficiency; FXPC-, premutation carriers without FXTAS; FXPC+, premutation carriers with FXTAS; FXTAS, fragile X-associated tremor/ataxia syndrome; MCP, middle cerebellar peduncle.

1. Introduction

The fragile X premutation is defined as a 55-200 CGG-repeat expansion in the non-coding region of *FMR1* gene (Hagerman *et al.*, 2001). A spectrum of clinical conditions are associated with the fragile X premutation, including neurodevelopmental and psychiatric problems, fragile X-associated primary ovarian insufficiency (FXPOI), and a late onset, progressive neurodegeneration disorder, fragile X-associated tremor/ataxia syndrome (FXTAS) (Hagerman and Hagerman, 2013). Among these conditions, FXTAS is particularly devastating, presenting with not only the core features of intention tremor and cerebellar gait ataxia, but also with additional features, including parkinsonism, peripheral neuropathy, cognitive deficits progressing to dementia, and problems in autonomic function, sensory perception, and immune regulation, in some patients (Hagerman and Hagerman, 2013). FXTAS shows a partial penetrance, affecting approximately 45% of male and 16.5% of female premutation carriers after age 50 (Rodriguez-Revenge *et al.*, 2009). An 'RNA toxic' gain-of-function model of FXTAS has been proposed based on the evidence that while *FMR1* protein (FMRP) is usually normal or moderately reduced, *FMR1* mRNA is significantly elevated in premutation carriers (Tassone *et al.*, 2000). The expanded CGG-containing mRNA sequesters RNA-binding proteins (e.g. Sam68, hnRNP A2, Drosha/DGCR8, etc.) that are important for normal cell functioning (Hagerman, 2012). In addition, it has been reported that repeat-associated non-ATG (RAN) translation may produce FMRpolyG that is toxic to premutation neurons both in human and animal models (Todd *et al.*, 2013, Oh *et al.*, 2015).

The cerebellum and brainstem are among the most affected brain areas in FXTAS. Both areas show intranuclear inclusions, the pathological hallmark of FXTAS, as well as white matter

disease (Greco *et al.*, 2002, Greco *et al.*, 2006). Radiological examinations reveal generalized brain atrophy and T2 signal hyperintensities in the middle cerebellar peduncle (MCP) and deep cerebral white matter in these patients (Brunberg *et al.*, 2002). MRI quantitative analyses highlight structural changes in the cerebellum and brainstem in premutation carriers both with (FXPC+) and without FXTAS (FXPC-), which may represent insipient structural changes before clinical manifestations arise (Cohen *et al.*, 2006, Hashimoto *et al.*, 2011, Battistella *et al.*, 2013, Leow *et al.*, 2014). However, all previously published studies were performed on adult premutation carriers. It is currently unknown whether the observed changes in FXPC- are part of an abnormal developmental process or part of a neurodegenerative process leading to FXTAS. Understanding the timing of atypical neuroanatomical changes in carriers will help to clarify diagnosis and prognosis and determine critical windows for effective therapeutic treatment.

To investigate whether cerebellar and brainstem changes are of developmental or neurodegenerative origin, we performed a large scale, cross-sectional neuroimaging analysis of 322 males from age 8 to 81 years. Cerebellar and brainstem volumes in these individuals were quantified to examine age-related changes in FXPC+ and FXPC-. The cerebellar and brainstem volume data were contrasted with whole brain and ventricular volumes to assess the contributions from the cerebellum and brainstem to overall brain atrophy. We also explored gene-brain-behavior relationships by studying the effect of FXTAS stage, CGG repeat length and *FMR1* mRNA level on brain volume measurements.

2. Material and methods

2.1 Research participants

We retrospectively inspected MRI scans acquired between 2007 and 2015, and selected 323 male participants who had usable high-resolution T1-weighted scans (Table 1). These comprised 142 healthy controls, 109 FXPC- and 72 FXPC+. All FXPC+ were older than age 50 except for a 34-year-old carrier who was at FXTAS stage 2. This participant was excluded in the analyses because he became an outlier in the regression models. Of the remaining 322 participants, 96 have been included in our previous studies (Wang *et al.*, 2012, Wang *et al.*, 2013a, Wang *et al.*, 2013b, Wang *et al.*, 2013c, Leow *et al.*, 2014). A trained physician (RJH) scored FXTAS severity for premutation carriers using the FXTAS stage. The categorization of premutation carriers according to FXTAS stage and age is presented in Table S1 in the appendix. Carriers with FXTAS stage 2 and above were classified as FXPC+. All participants provided written consent and research was conducted following procedures approved by the UC Davis Institutional Review Board.

2.2 Molecular Genetic Data

Genomic DNA was isolated from peripheral blood lymphocytes using standard method (Qiagen, Valencia, CA). CGG repeat size was determined using a combination of PCR and Southern blot Analysis as previously described (Tassone *et al.*, 2008, Filipovic-Sadic *et al.*, 2010). For seven out of 180 premutation carriers who had two alleles, the larger alleles were used for the analyses. Total cellular RNA was purified from 2.5 ml peripheral blood. *FMR1* mRNA expression levels were measured by quantitative Real Time PCR using a 7900 Sequence

detector (PE Biosystems) as previously described (Tassone *et al.*, 2000). Two RNA extraction methods were used chronologically, resulting in differences in measurements. To combine the data, we utilized mRNA levels measured from 24 participants (10 controls, 14 premutation carriers) using both methods (mean 1.92 ± 0.87 vs. 0.73 ± 0.32), which showed high correlation ($r = 0.79$, 95% confidence interval [0.57, 0.91], $p < 0.001$). We calculated z-scores based on these data for subsequent analyses.

2.3 MRI acquisitions

High-resolution T1-weighted MPRAGE images were acquired on a Siemens Trio 3T MRI scanner (Siemens Medical Solutions, Erlangen, Germany). Over the 9 years of image acquisition, there was a scanner upgrade in late 2009 followed by a switch of the head coil from 8- to 32-channel in early 2010. Scans were collected by four different research projects using two different imaging protocols. About one-third of the scans have image resolution $0.47 \times 0.47 \times 0.95 \text{ mm}^3$ and two-thirds $1 \times 1 \times 1 \text{ mm}^3$ (Table S2).

2.4 MRI Analyses

We segmented the cerebellum and brainstem semi-automatically following our published method (Wang *et al.*, 2016). Briefly, the initial segmentation was generated automatically using FreeSurfer 5.3.0 (<http://freesurfer.net/>) (Fischl *et al.*, 2002) where image resolutions were conformed to $1 \times 1 \times 1 \text{ mm}^3$. We then used a machine-learning based tool, SegAdapter (<http://www.nitrc.org/projects/segadapter/>) (Wang *et al.*, 2011) to extend the brainstem boundary to include substantia nigra as well as to correct segmentation errors such

as inclusions of neurocortex, CSF and bone marrow and incomplete labeling of the cerebellum and brainstem. Finally, we corrected remaining errors using ITK-Snap (<http://www.itksnap.org/>). The manual correction was performed blind to the status of the participants. Figure 1 A-C shows representative cerebellum and brainstem segmentations. Mask generation and volume calculation were conducted using command tools `fslmaths` and `fslstats`, respectively, from FSL (<http://fsl.fmrib.ox.ac.uk/fsl/fslwiki/>).

To assess the contributions from the cerebellum and brainstem to overall brain atrophy, we quantified whole brain volume and ventricular size using an automated FSL tool (<http://fsl.fmrib.ox.ac.uk/fsl/fslwiki/>), SIENAX (Smith, 2002). Before the processing, MRI scans with image resolution of $0.47 \times 0.47 \times 0.95 \text{ mm}^3$ were resliced to $1 \times 1 \times 1 \text{ mm}^3$ using the `mri_convert` command from FreeSurfer and MRI bias field correction was performed on all scans using N4 from ANT (<http://stnava.github.io/ANTs/>) (Tustison *et al.*, 2010). Results were checked for accuracy and input parameter for brain extraction was adjusted for optimal results. We found that cavum vergae (CV) and cavum septum pellucidum (CSP) were mislabeled as ventricles, and the premutation carriers had a significantly higher prevalence of large CSP (spanning $\geq 6 \text{ mm}$ in the coronal direction) (Takahashi *et al.*, 2008) compared to the controls (13.9% vs. 5.6%, odds ratio = 2.70, $p = 0.019$, Table S3). Since small CSP ($1\text{-}5 \text{ mm}^3$) had trivial effect on ventricular volumes, we quantified large CSP and CV using ITK-Snap and subtracted the volumes from ventricular volumes (Fig. S1).

Figure S2 A-D in the Appendix depicts age-related volume changes. To account for the effect of head size variation on volumetric data, we used brain scaling factor calculated by SIENAX, in all statistical analyses. During estimations of brain tissue volumes, SIENAX generates

the brain and skull images from whole head image data, and utilizes the brain and external skull images for affine-transformation to a standard space. The brain scaling factor is then computed as the determinant of the affine transformation and used as a scaling factor for normalizing the head size (Smith, 2002). Brain scaling factor has shown high correlation to manual total cranial volume previously (Buckner *et al.*, 2004) and is less affected by aging compared to total cranial volume (Fig. S2 E-F).

2.5 Statistical analyses

We performed multiple regression to evaluate age and group effects, and their interaction, on brain volume data. We inspected the residuals to evaluate fit of the regression models to the data. Since all FXPC+ were older than age 50 except for a 34-year-old carrier who was at FXTAS stage 2 (excluded because he was an outlier in the regression models), FXPC+ was compared to age-matched controls and FXPC- (i.e. age > 50, Table 1). Age was centered at the youngest age for each comparison. Multiple regression was also conducted for predicting volumetric data using age, FXTAS stage, CGG repeat size and *FMR1* mRNA level. Previous cross-sectional and longitudinal studies of aging reported non-linear volume changes in the cerebellum, brainstem, and ventricles (Raz *et al.*, 2005, Walhovd *et al.*, 2011, Fjell *et al.*, 2013). Scanner upgrade, the change of head coil from 8-channel to 32-channel and the utilizations of two different MRI acquisition protocols may affect image signal-to-noise (SNR) ratio. To account for potential biases caused by these variabilities as well as non-linear age-related changes in volumes, covariates including scanner upgrade, head coil usage, and image resolution along with age-squared were included in regression models whenever significant. Benjamini-

Hochberg method of false discovery rate (Benjamini and Hochberg, 1995) was used to correct for multiple comparisons. The open-source statistical package R (<http://www.r-project.org/>) was used for statistical analyses.

3. Results

3.1 Abnormal trajectories of brain volume measurements in FXPC-

In both control and FXPC- groups, volumes of cerebellum and whole brain decreased linearly with age, while brainstem volumes displayed an inverted U-shaped change with age, and the ventricular volumes exhibited quadratic curves that increased monotonically (Fig. 1D). Compared to the controls, FXPC- displayed significantly larger ventricles, and significant age and group interactions in cerebellar, brainstem, and whole brain volumes (Table 2). Specifically, FXPC- showed faster age-related decrease in cerebellar volumes (0.51 vs. 0.36 ml/year) and whole brain volumes (4.59 vs. 3.66 ml/year). In controls, brainstem volumes showed a protracted developmental trajectory that peaked at 32.6 ml at age 44.9 years, a 5.53% increase from age 8. In contrast, FXPC- had a flat developmental trajectory that peaked at 31.1 ml at age 23.4 years, a 0.52% increase from age 8. For the four covariates included in the regression models, only brain scaling factor showed as a significant predictor for all volume data ($t = -21.5$ to -6.01 , $p < 0.001$). The other three covariates, namely scanner upgrade, head coil, and image resolution did not show as significant predictors for volumes, nor did their inclusions affect the results. Since brain scaling factor had a significant effect on the brain volume data, the estimations of the peak brainstem volume were calculated using the average brain scaling of all participants, which was 1.221. Based on these predicted trajectories, we estimated that the

volume divergence between controls and FXPC- became significant around age 28 for the brainstem, age 30 for the cerebellum, and age 40 for whole brain (Table S4).

To determine whether the age-related changes in cerebellar and brainstem volumes were disproportional to whole brain volume, we added whole brain volume as an additional covariate in the regression models. While the age \times group interaction effect remained significant for brainstem volume ($\beta = -0.036$, $p = 0.024$), the interaction was not significant for cerebellar volume. In contrast, the cerebellum was significantly smaller ($\beta = -3.74$, $p = 0.003$) in FXPC- compared to the controls after controlling for whole brain volume.

3.2 Brain volume atrophy plus accelerated volume atrophy in FXPC+

All volumetric data exhibited linear relationships with age in the older groups (Table 2; Fig. 1E). With age centered at 50 years, FXPC+ showed significant differences from the controls in volumes of ventricles (21.0 ml higher), cerebellum (23.7 ml lower), brainstem (4.77 ml lower), and whole brain (109.7 ml lower). FXPC+ also showed significant volume differences in the cerebellum (14.1 ml lower) and whole brain (72.0 ml lower) compared to FXPC-. With respect to annual rates of volume changes, FXPC+ exhibited accelerated age-related brainstem atrophy compared to both controls and FXPC- (0.22 ml/year decrease vs. 0.07 ml/year decrease for the controls and 0.09 ml/year increase for FXPC-) and accelerated ventricular volume increase (1.52 ml/year vs. 0.13 ml/year) compared to FXPC-. By contrast, the annual rates of volume changes in the cerebellum and whole brain were not statistically different between the three groups.

Similar to the comparisons between FXPC- and healthy controls, brain scaling factor was

the only covariate that showed as significant for all brain volume data ($t = -16.3$ to -6.65 , $p < 0.001$) when comparing the FXPC+ group to the control and FXPC- groups. The other three covariates, namely scanner upgrade, head coil, and image resolution, did not have significant effects on the findings

We also included whole brain volume as an additional covariate to determine whether the observed changes in the cerebellar and brainstem volumes were disproportional to overall brain volume changes. The group effect in the cerebellar volume and age \times group interaction effect in the brainstem volume remained significant between FXPC+ and the other two groups after controlling for whole brain volumes ($t = 3.24 - 10.31$, $p = < 0.001 - 0.001$).

3.3 FXTAS stage and molecular measurements are significant predictors of brain volume measurements

CGG repeat length had a quadratic relation with *FMR1* mRNA level in the premutation carriers ($R_{Adj} = 0.61$, $df = 171$, $p < 0.001$, Fig. S3) while no relation was observed in healthy controls ($r = 0.05$, $df = 130$, $p = 0.61$). In the analyses of using FXTAS stage (for premutation carriers only) and molecular measurements to predict volumetric data while adjusting for age and brain scaling factor, FXTAS stage, CGG, and CGG-squared were significant predictors for all volumetric data in the premutation carriers, whereas *FMR1* mRNA level was a significant predictor for whole brain volume in the controls (Table 3). FXTAS stage was negatively correlated with cerebellar, brainstem, and whole brain volumes and positively correlated with ventricular volume. CGG repeat length exhibited U-shaped relationships with cerebellar, brainstem and whole brain volumes, and an inverted U-shaped relationship with ventricular

volume in the premutation carriers (Fig. 2). In comparison, the controls displayed a negative linear relationship between *FMR1* mRNA and whole brain volume after adjusting for age and brain scaling factor (Fig. S4).

We further examined the relationships between FXTAS stage and brain volume measurements treating FXTAS stage as a categorical variable. The results showed that the most significant changes in cerebellar and brainstem volumes occurred between FXTAS stage 2 and 3 and between FXTAS stage 3 and 4 (Table S5).

4. Discussion

This study demonstrated abnormal age-related brain volume trajectories in the cerebellum, brainstem, ventricles and whole brain in fragile X premutation carriers, both with and without a diagnosis of FXTAS (FXPC+ and FXPC-). The brain volume measurements also significantly correlated with FXTAS stage and CGG repeat length in these premutation carriers after controlling for age and brain scaling factor.

With age centered at the youngest age of 8 years, the FXPC- group did not show a significant group difference in cerebellar volume compared to the controls; however, they demonstrated a faster age-related decrease in cerebellar volume. The regression model fitting the data suggests that the process may begin during young adulthood. This is decades before the average age of FXTAS onset in males at 62.6 years (Tassone *et al.*, 2007) and raises an important question about whether the faster volume decrease is driven by the premutation status common to all carriers or by the neurological disease process affecting a subset of carriers that will go on to develop FXTAS. The result of significantly atrophied cerebellum in

FXPC+ compared to both age-matched controls and FXPC- (with age centered at 50) indicates the potential occurrence of cerebellar atrophy in FXPC+ prior to their clinical diagnoses.

Unexpectedly, the cerebellar atrophy rate was not significantly different in FXPC+ relative to the other two groups of healthy controls and FXPC- older than 50. The findings from the FXPC- and FXPC+ groups suggest that faster than normal decline in cerebellar volume may start early in young adulthood in some FXPC- and the volume decrease appears to accumulate slowly over the decades before the clinical presentation of FXTAS. Longitudinal studies are needed to confirm these observations.

The cerebellum has been postulated to play a critical role in the maturation of functional networks with neocortex (Wang *et al.*, 2014). The cerebellum maintains functionally segregated, reciprocal connections with almost all areas in the neocortex. It generates internal models for behaviors, and guides the neocortex to store the most efficient representations for movement and high level cognitive and emotional processing (Koziol *et al.*, 2012). Subtle underdevelopment of the cerebellum may underlie developmental problems, including autism, anxiety and deficits in attention and visual motion processing that have been documented in children with fragile X premutation (Farzin *et al.*, 2006, Gallego *et al.*, 2014, Cordeiro *et al.*, 2015) as well as motor impairment in FXPC- (O'Keefe *et al.*, 2015). In FXTAS cerebellar structural damage becomes clinically observable, with MRI signal hyperintensities in the MCP being used as a diagnostic criterion (Brunberg *et al.*, 2002). The central role of cerebellum in FXTAS pathology is further highlighted by the evidence of a negative relationship between cerebellar volume and postural sway (Birch *et al.*, 2015) and the associations of superior cerebellar

peduncle with behavioral regulation and fine motor skills in premutation carriers (Wang *et al.*, 2013c).

Several factors can contribute to the high vulnerability of the cerebellum to FXTAS pathology. First, the cerebellum has a protracted developmental course that reaches its peak volume during late childhood or adolescence (Tiemeier *et al.*, 2010). Brain structures are vulnerable to environmental toxicities especially when they are in the active processes of cell proliferation and myelination during development. Early life perturbation such as seizure and exposure to toxins may predispose the cerebellum to accelerated aging later in life (Rice and Barone, 2000). Second, the cerebellum is metabolically active and is involved in a variety of tasks as shown by functional MRI studies (Koziol *et al.*, 2014). The high metabolic rate may contribute to cerebellar vulnerability to mitochondrial dysfunction, RNA toxicity, environmental insults, and comorbidity, and thus increase its risk of atrophy during aging. Indeed, intranuclear inclusions have been observed in dentate nuclei, reflecting the effect of RNA toxicity; and mitochondrial dysfunction (Ross-Inta *et al.*, 2010, Napoli *et al.*, 2016) and high prevalence of hypertension, substance abuse and alcohol abuse have been reported in premutation carriers (Dorn *et al.*, 1994, Kogan *et al.*, 2008, Polussa *et al.*, 2014), which may play a role in cerebellar atrophy during aging (Miquel *et al.*, 2009, Lavezzi *et al.*, 2013, Miquel *et al.*, 2016). Additional studies are needed to uncover the mechanisms causing cerebellar underdevelopment often with specific developmental problems and late neurodegeneration due to FXTAS progression.

In the brainstem, FXPC- displayed an early maturation at age 23.4 years, about two decades earlier than controls that experienced a protracted maturation that peaked at age 44.9 years (Fig. 1D). The early divergence in developmental trajectories between the two groups is

consistent with previous findings of decreased brainstem volume in young (age 18-44) (Leow *et al.*, 2014) and older (age 51-79) (Cohen *et al.*, 2006) FXPC-. In comparison, FXPC+ exhibited significantly smaller brainstem volume compared to the older controls, and accelerated volume loss compared to both older controls and older FXPC-. Thus, the divergence of brainstem volume in FXPC+ from healthy controls occurred before age 50, while the divergence from FXPC- emerged after age 50. Importantly, the age-related changes in brainstem volume for both FXPC- and FXPC+ were disproportional to overall brain volume change since these effects remained significant after controlling for whole brain volume. However, the brainstem is a complex structure containing various life-sustaining nuclei and fiber tracts connecting the cerebrum, cerebellum, and spinal cord. We cannot rule out the possibility that regional brainstem measurements (e.g. cerebellar peduncles) may differentiate FXPC+ from FXPC- before age 50. In addition, certain brainstem structures may be proven important for FXTAS phenotypic representations such as parkinsonism (Scaglione *et al.*, 2008), sensorineural hearing loss (Juncos *et al.*, 2011) and eye movement impairment (Fraint *et al.*, 2014). Further segmentation of the brainstem is needed to determine whether specific structures within the brainstem show prodromal signs of FXTAS.

Of the four measurements (i.e., volumes of the cerebellum, brainstem, whole brain and ventricles), only ventricular volume showed a significant group difference between FXPC- and controls with no difference in age-related rate of volume increase. In FXPC+, the rate of volume increase became significantly higher compared to both controls and FXPC-. These results implicate the sensitivity of ventricular volume to brain abnormalities during both neurodevelopment and FXTAS progression. Factors influencing ventricular size include

cerebrospinal fluid (CSF) dynamics, abnormally developed brain structures, brain atrophy and variable distribution of CSF between ventricles and sulci (Sarwar, 1989, Scahill *et al.*, 2003).

Given the findings of intranuclear inclusions in neurons, astrocytes, ependymal cells and choroid plexus cells in FXPC+ (Greco *et al.*, 2006), it is important to assess whether the CSF regulatory functions are affected in those with the fragile X premutation.

The current study is limited by studying only gross volumes, which may not be sensitive to regional volume changes or other types of structural changes not reflected in volumetric measurements. The current study is also cross-sectional and requires confirmation from longitudinal analyses. While findings from cross-sectional studies can serve as important basis for the design of longitudinal studies, it cannot be used for inferring within-person trajectories. Most importantly, there is no information of within-person changes in cross-section data. Thus individual differences in the slope cannot be estimated (Miyazaki and Raudenbush, 2000). Several factors (Kraemer *et al.*, 2000) can cause variability in within-person trajectories, which can lead to discordance between within-person trajectories and slope estimated from cross-sectional data. First, the age of onset of FXTAS is not fixed, with a median age of onset at about 60 years (Leehey *et al.*, 2007). Although it remains to be established, patients with earlier onset may have more severe brain atrophy than those with later onset. Second, life expectancy for FXPC+ varies, with a range of 5-25 years (Leehey *et al.*, 2007). Thus patients may progress in different speed and present with different rate of brain atrophy. Finally, reliability of the measurements can also affect the estimations of slopes in both cross-sectional and longitudinal data. We have included some preliminary longitudinal data in Figure S5 to provide a glimpse of how longitudinal data may look like. In addition, segmentation may be improved by using

multimodal imaging processing. This improvement, however, relies on accurate co-registration between scans acquired using different MRI techniques and whether the new image modality provides increased tissue contrasts for the structure of interest.

The relevance of the brain volume measurements to clinical observation and molecular mechanisms is demonstrated in their significant linear relations with FXTAS stage and nonlinear relations with CGG repeat length. Inverted U-shaped relation between CGG repeat length and MCP packing density has been observed in male premutation carriers (Hashimoto *et al.*, 2011) as well as U-shaped relations between CGG repeat length and psychological problems and menopausal age in females with the premutation (Loesch *et al.*, 2015). These non-linear CGG effects indicate the heightened RNA-toxicity of mid-size repeats, although the underlying molecular mechanisms remain to be explored. A significant negative relation between *FMR1* mRNA and whole brain volume was also discovered in the controls with normal alleles. This parallels with our previously reported negative association between *FMR1* mRNA and white matter integrity in male controls (Wang *et al.*, 2013b), suggesting that high levels of *FMR1* mRNA may be suboptimal for brain structures even in healthy individuals from the general population.

In summary, we revealed accelerated age-related volume decreases in the cerebellum and brainstem, and increased ventricular volume in FXPC- compared to controls. While FXPC+ showed significant volume changes in all four measurements relative to the controls, only cerebellar and whole brain volumes were significantly lower compared to the FXTAS- at age 50, suggesting the potential utilities of these two measurements for premutation neurological monitoring and FXTAS prognosis. Significant associations between CGG repeat length and brain

volume measurements support the notion that expanded CGG length may contribute to the abnormal age-related changes in cerebellar and brainstem volumes and enlarged ventricles during early life, an effect that becomes much more prominent during aging in fragile X premutation carriers.

Acknowledgements

We are grateful to the research participants and their families; to Vivien Narcissa, Cindy Johnston, Floridette Abucayan, and Jessica Famula for participant recruitment; to John Wang, Patrick Adams, Yingratana Amabel McLennan, and Emily Halket for neuroimaging data collection; and Michael Ngo, Jihyun Park, Bhavana Rai, and Riley Swift for performing segmentation. This project was supported by PhRMA Foundation TMT Fellowship, NIH grants MH078041, HD036071 and the MIND Institute Intellectual and Developmental Disabilities Research Center U54 HD079125. Dr. Hagerman has received funding from Novartis, Roche Pharmaceuticals, Alcobra and Neuren to carry out treatment studies in fragile X syndrome. She has also consulted with Roche/Genetech, Zynerba, Ovid, Neuren and Novartis regarding treatment studies in fragile X syndrome. Dr Hessler has received funding from Novartis, Roche and Seaside Therapeutics for consultation regarding treatment studies in fragile X syndrome.

Tables

Table 1. Primary molecular and brain volume measurements: mean (SD).

Characteristics	<i>N</i>	Controls Age 8-81	<i>N</i>	FXPC- Age 8-75	<i>N</i>	FXPC+ Age 50-79	<i>N</i>	Older Controls Age 50-81	<i>N</i>	Older FXPC- Age 50-75
Age (years)	142	44.6 (20.9)	109	40.7 (20.4)	71	66.6 (6.7)	68	63.7 (7.9)	42	62.4 (6.5)
<i>FMR1</i> CGG repeat size	139	29.4 (4.7)	109	94.1 (32.1)	70	94.2 (16.8)	65	28.9 (4.6)	42	83.7 (22.8)
<i>FMR1</i> mRNA level**	132	-0.69 (0.31)	105	1.10 (1.38)	68	1.17 (0.95)	64	-0.69 (0.32)	41	0.66 (1.10)
Cerebellar volume (ml)	142	132.6 (13.0)	109	129.8 (14.8)	71	102.3 (13.5)	68	126.5 (11.2)	42	119.3 (13.1)
Brainstem volume (ml)	142	31.9 (3.3)	109	30.4 (3.2)	71	24.9 (3.4)	68	32.1 (3.0)	42	29.5 (3.6)
Ventricular volume (ml)	142	33.1 (15.3)	109	36.4 (20.0)	71	76.3 (25.1)	68	42.5 (14.0)	42	52.5 (19.3)
Whole brain volume (l)	142	1.26 (0.11)	109	1.27 (0.12)	71	1.10 (0.10)	68	1.20 (0.10)	42	1.19 (0.09)

Abbreviations: FXPC-, fragile X premutation carriers without fragile X-associated tremor/ataxia syndrome; FXPC+, fragile X premutation carriers with fragile X-associated tremor/ataxia syndrome.

Table 2. The effect of group and group \times age on brain volume measurements.

Measurements	FXPC- Vs. Controls			Older Controls Vs. FXPC+*			Older FXPC- Vs. FXPC+*	
	$R_{Adj.}$	β (SE) (ml)	P	$R_{Adj.}$	β (SE) (ml)	P	β (SE) (ml)	P
<i>Cerebellar volume</i>	0.43		< 0.001	0.56		< 0.001		< 0.001
Age		-0.36 (0.04)	< 0.001		-0.52 (0.11)	< 0.001	-0.52 (0.11)	< 0.001
Group		-0.18 (2.58)	0.94		23.7 (1.89)	< 0.001	14.1 (2.19)	< 0.001
Age \times group		-0.15 (0.06)	0.017		-	-	-	-
<i>Brainstem volume</i>	0.34		< 0.001	0.63		< 0.001		< 0.001
Age squared		-0.001 (0.0005)	0.009		-	-	-	-
Age		0.093 (0.036)	0.010		-0.22 (0.05)	< 0.001	-0.22 (0.05)	< 0.001
Group		-0.068 (0.67)	0.92		4.77 (1.11)	< 0.001	-0.44 (1.29)	0.730
Age \times group		-0.054 (0.017)	0.002		0.15 (0.07)	0.023	0.31 (0.08)	< 0.001
<i>Ventricular volume</i>	0.52		< 0.001	0.59		< 0.001		< 0.001
Age squared		0.006 (0.002)	0.007		-	-	-	-
Age		0.107 (0.15)	0.48		1.52 (0.30)	< 0.001	1.52 (0.30)	< 0.001
Group		4.73 (1.67)	0.003		-21.0 (6.75)	0.002	-3.67 (7.82)	0.64
Age \times group		-	-		-0.69 (0.40)	0.09	-1.39 (0.51)	0.007
<i>Whole brain volume</i>	0.75		< 0.001	0.69		< 0.001		< 0.001
Age		-3.66 (0.23)	< 0.001		-3.43 (0.63)	< 0.001	-3.43 (0.63)	< 0.001
Group		13.2 (14.2)	0.35		109.7 (10.4)	< 0.001	72.0 (44.3)	< 0.001
Age \times group		-0.93 (0.36)	0.009		-	-	-	-

Abbreviations: FXPC-, fragile X premutation carriers without fragile X-associated tremor/ataxia syndrome; FXPC+, fragile X premutation carriers with fragile X-associated tremor/ataxia syndrome.

Bold, significant at 5% false discovery rate.

* The comparisons of FXPC+ with older controls and FXPC- were performed in the same regression analyses.

Table 3. The effect of FXTAS stage, CGG repeat length, and *FMR1* mRNA on volume measurements.

Measurements	Cerebellum			Brainstem			Ventricles			Whole Brain		
	<i>R</i> _{Adj.}	β (SE) (ml)	<i>P</i>	<i>R</i> _{Adj.}	β (SE) (ml)	<i>P</i>	<i>R</i> _{Adj.}	β (SE) (ml)	<i>P</i>	<i>R</i> _{Adj.}	β (SE) (ml)	<i>P</i>
<i>FXPC</i> (<i>N</i> = 179)	0.70		< 0.001	0.59		< 0.001	0.73		< 0.001	0.81		< 0.001
Age-squared		-	-		-0.001 (0.001)	0.033		0.010 (0.004)	0.008		-	-
Age		-0.51 (0.05)	< 0.001		0.041 (0.044)	0.36		-0.10	0.68		4.39 (0.31)	< 0.001
FXTAS stage		-4.57 (0.69)	< 0.001		-1.19 (0.19)	< 0.001		-6.98 (1.10)	< 0.001		-21.0 (3.9)	< 0.001
CGG-squared		0.002 (0.001)	0.030		0.001 (0.0002)	0.008		-0.003 (0.001)	0.005		0.011 (0.004)	0.014
CGG		-0.41 (0.17)	0.018		-0.13 (0.04)	0.003		0.78 (0.26)	0.003		-3.08 (0.10)	0.015
<i>HC</i> (<i>N</i> = 132)	0.39		< 0.001	0.36		< 0.001	0.59		< 0.001	0.76		< 0.001
Age-squared		-	-		-0.002 (0.001)	0.003		0.007 (0.002)	0.005		-	-
Age		-0.37 (0.05)	< 0.001		0.135 (0.046)	0.004		-0.002 (0.172)	0.99		-3.54 (0.23)	< 0.001
<i>FMR1</i> mRNA		-3.35 (2.99)	0.27		-1.11 (0.76)	0.15		2.38 (2.84)	0.40		-35.0 (15.0)	0.021

Abbreviations: FXPC, fragile premutation carriers; HC, healthy control

Bold, significant at 5% false discovery rate.

Figure Legends**Fig. 1. Samples of segmented cerebellum and brainstem and plots of age-related volume**

changes. Segmented cerebellum and brainstem from (A) a 68-year-old healthy control, (B) a 69-year-old premutation carrier at FXTAS stage 1, and (C) a 68-year-old premutation carrier at FXTAS stage 4. Scatter plots showing age-related changes in cerebellar, brainstem, and ventricular volumes in (D) premutation carriers without FXTAS (FXPC-, at FXTAS stage 0 or 1) and healthy controls and (E) older groups (age > 50 years).

Fig. 2. The effect of FXTAS stage and molecular measurements on brain volumes in

premutation carriers. (A) Cerebellar volume, (B) brainstem volume, (C) ventricular volume, and (D) whole brain volume. For FXTAS stage, brain volumetrics adjusted for age and brain scaling factor are shown. For CGG repeat length and *FMR1* mRNA, brain volumetrics adjusted for age, brain scaling factor and FXTAS stage are shown. Shaded areas represent 95% confidence intervals of the regression lines.

References

- Battistella G, Niederhauser J, Fornari E, Hippolyte L, Gronchi Perrin A, Lesca G, Forzano F, Hagmann P, Vingerhoets FJ, Draganski B, Maeder P, Jacquemont S. Brain structure in asymptomatic FMR1 premutation carriers at risk for fragile X-associated tremor/ataxia syndrome. *Neurobiol Aging* 2013; 34: 1700-7.
- Benjamini Y, Hochberg Y. Controlling the False Discovery Rate - a Practical and Powerful Approach to Multiple Testing. *J R Statist Soc B* 1995; 57: 289-300.
- Birch RC, Hocking DR, Cornish KM, Menant JC, Georgiou-Karistianis N, Godler DE, Wen W, Hackett A, Rogers C, Trollor JN. Preliminary evidence of an effect of cerebellar volume on postural sway in FMR1 premutation males. *Genes, brain, and behavior* 2015; 14: 251-9.
- Brunberg JA, Jacquemont S, Hagerman RJ, Berry-Kravis EM, Grigsby J, Leehey MA, Tassone F, Brown WT, Greco CM, Hagerman PJ. Fragile X premutation carriers: characteristic MR imaging findings of adult male patients with progressive cerebellar and cognitive dysfunction. *AJNR Am J Neuroradiol* 2002; 23: 1757-66.
- Buckner RL, Head D, Parker J, Fotenos AF, Marcus D, Morris JC, Snyder AZ. A unified approach for morphometric and functional data analysis in young, old, and demented adults using automated atlas-based head size normalization: reliability and validation against manual measurement of total intracranial volume. *Neuroimage* 2004; 23: 724-38.
- Cohen S, Masyn K, Adams J, Hessel D, Rivera S, Tassone F, Brunberg J, DeCarli C, Zhang L, Cogswell J, Loesch D, Leehey M, Grigsby J, Hagerman PJ, Hagerman R. Molecular and imaging correlates of the fragile X-associated tremor/ataxia syndrome. *Neurology* 2006; 67: 1426-31.
- Cordeiro L, Abucayan F, Hagerman R, Tassone F, Hessel D. Anxiety disorders in fragile X premutation carriers: Preliminary characterization of probands and non-probands. *Intractable & rare diseases research* 2015; 4: 123-30.

- Dorn MB, Mazzocco MM, Hagerman RJ. Behavioral and psychiatric disorders in adult male carriers of fragile X. *Journal of the American Academy of Child and Adolescent Psychiatry* 1994; 33: 256-64.
- Farzin F, Perry H, Hessler D, Loesch D, Cohen J, Bacalman S, Gane L, Tassone F, Hagerman P, Hagerman R. Autism spectrum disorders and attention-deficit/hyperactivity disorder in boys with the fragile X premutation. *J Dev Behav Pediatr* 2006; 27: S137-44.
- Filipovic-Sadic S, Sah S, Chen L, Krosting J, Sekinger E, Zhang W, Hagerman PJ, Stenzel TT, Hadd AG, Latham GJ, Tassone F. A novel FMR1 PCR method for the routine detection of low abundance expanded alleles and full mutations in fragile X syndrome. *Clin Chem* 2010; 56: 399-408.
- Fischl B, Salat DH, Busa E, Albert M, Dieterich M, Haselgrove C, van der Kouwe A, Killiany R, Kennedy D, Klaveness S, Montillo A, Makris N, Rosen B, Dale AM. Whole brain segmentation: automated labeling of neuroanatomical structures in the human brain. *Neuron* 2002; 33: 341-55.
- Fjell AM, Westlye LT, Grydeland H, Amlie I, Espeseth T, Reinvang I, Raz N, Holland D, Dale AM, Walhovd KB, Alzheimer Disease Neuroimaging I. Critical ages in the life course of the adult brain: nonlinear subcortical aging. *Neurobiol Aging* 2013; 34: 2239-47.
- Fraint A, Vittal P, Szewka A, Bernard B, Berry-Kravis E, Hall DA. New observations in the fragile X-associated tremor/ataxia syndrome (FXTAS) phenotype. *Frontiers in genetics* 2014; 5: 365.
- Gallego PK, Burris JL, Rivera SM. Visual motion processing deficits in infants with the fragile X premutation. *Journal of neurodevelopmental disorders* 2014; 6: 29.
- Greco CM, Berman RF, Martin RM, Tassone F, Schwartz PH, Chang A, Trapp BD, Iwahashi C, Brunberg J, Grigsby J, Hessler D, Becker EJ, Papazian J, Leehey MA, Hagerman RJ, Hagerman PJ. Neuropathology of fragile X-associated tremor/ataxia syndrome (FXTAS). *Brain* 2006; 129: 243-55.

Greco CM, Hagerman RJ, Tassone F, Chudley AE, Del Bigio MR, Jacquemont S, Leehey M, Hagerman PJ.

Neuronal intranuclear inclusions in a new cerebellar tremor/ataxia syndrome among fragile X carriers. *Brain* 2002; 125: 1760-71.

Hagerman PJ. Current Gaps in Understanding the Molecular Basis of FXTAS. *Tremor Other Hyperkines Mov (N Y)* 2012; 2.

Hagerman R, Hagerman P. Advances in clinical and molecular understanding of the FMR1 premutation and fragile X-associated tremor/ataxia syndrome. *Lancet neurology* 2013; 12: 786-98.

Hagerman RJ, Leehey M, Heinrichs W, Tassone F, Wilson R, Hills J, Grigsby J, Gage B, Hagerman PJ. Intention tremor, parkinsonism, and generalized brain atrophy in male carriers of fragile X. *Neurology* 2001; 57: 127-30.

Hashimoto R, Srivastava S, Tassone F, Hagerman RJ, Rivera SM. Diffusion tensor imaging in male premutation carriers of the fragile X mental retardation gene. *Mov Disord* 2011; 26: 1329-36.

Juncos JL, Lazarus JT, Graves-Allen E, Shubeck L, Rusin M, Novak G, Hamilton D, Rohr J, Sherman SL. New clinical findings in the fragile X-associated tremor ataxia syndrome (FXTAS). *Neurogenetics* 2011; 12: 123-35.

Kogan CS, Turk J, Hagerman RJ, Cornish KM. Impact of the Fragile X mental retardation 1 (FMR1) gene premutation on neuropsychiatric functioning in adult males without fragile X-associated Tremor/Ataxia syndrome: a controlled study. *Am J Med Genet B Neuropsychiatr Genet* 2008; 147B: 859-72.

Koziol LF, Budding D, Andreasen N, D'Arrigo S, Bulgheroni S, Imamizu H, Ito M, Manto M, Marvel C, Parker K, Pezzulo G, Ramnani N, Riva D, Schmahmann J, Vandervort L, Yamazaki T. Consensus paper: the cerebellum's role in movement and cognition. *Cerebellum* 2014; 13: 151-77.

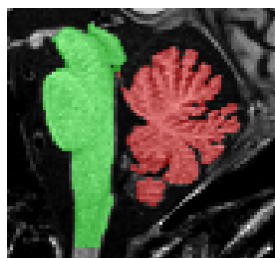
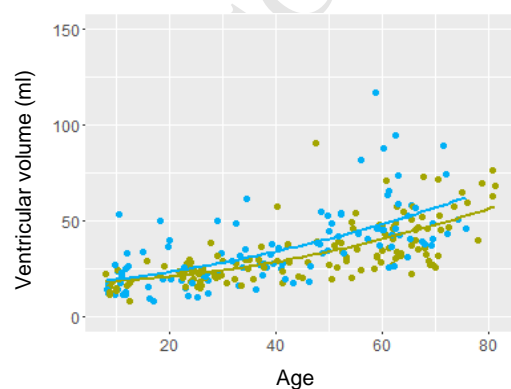
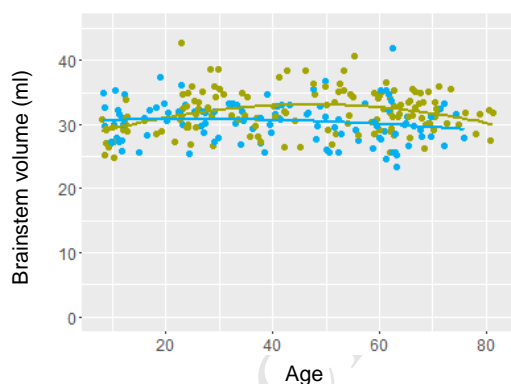
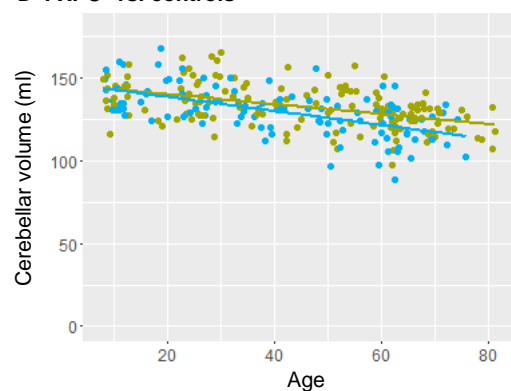
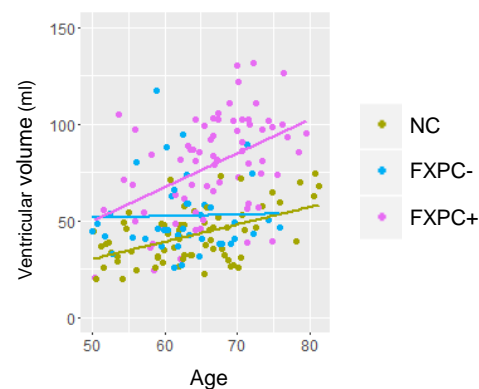
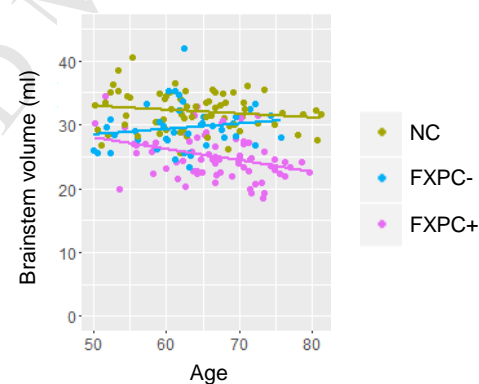
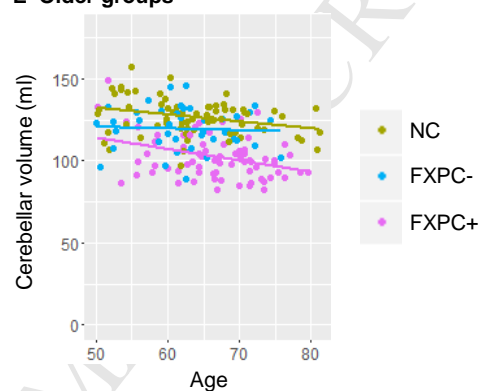
Koziol LF, Budding DE, Chidekel D. From movement to thought: executive function, embodied cognition, and the cerebellum. *Cerebellum* 2012; 11: 505-25.

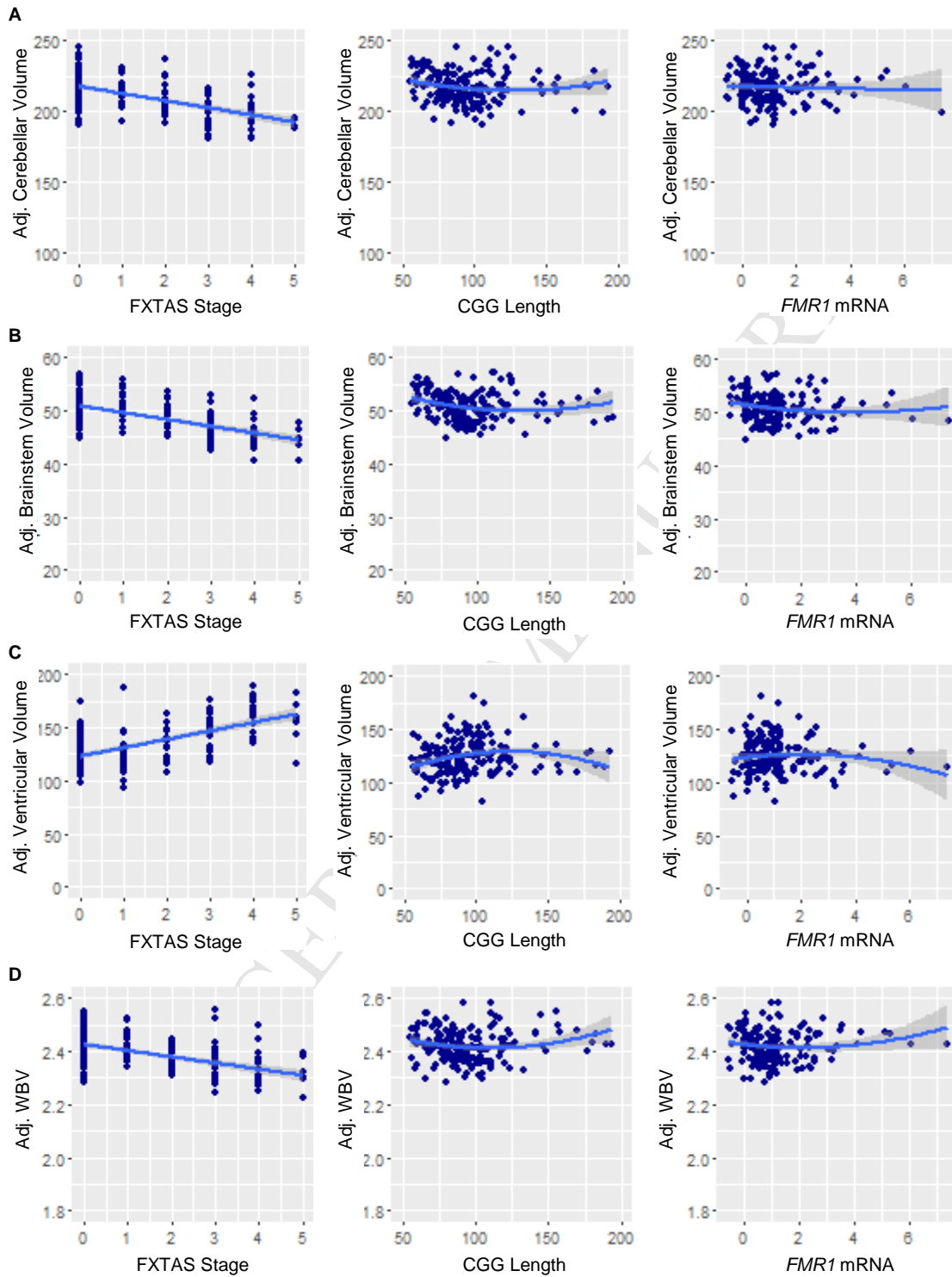
- Kraemer HC, Yesavage JA, Taylor JL, Kupfer D. How can we learn about developmental processes from cross-sectional studies, or can we? *Am J Psychiatry* 2000; 157: 163-71.
- Lavezzi AM, Corna MF, Repetti ML, Matturri L. Cerebellar Purkinje cell vulnerability to prenatal nicotine exposure in sudden unexplained perinatal death. *Folia Neuropathol* 2013; 51: 290-301.
- Leehey MA, Berry-Kravis E, Min SJ, Hall DA, Rice CD, Zhang L, Grigsby J, Greco CM, Reynolds A, Lara R, Cogswell J, Jacquemont S, Hessler DR, Tassone F, Hagerman R, Hagerman PJ. Progression of tremor and ataxia in male carriers of the FMR1 premutation. *Mov Disord* 2007; 22: 203-6.
- Leow A, Harvey D, Goodrich-Hunsaker NJ, Gadelkarim J, Kumar A, Zhan L, Rivera SM, Simon TJ. Altered structural brain connectome in young adult fragile X premutation carriers. *Hum Brain Mapp* 2014; 35: 4518-30.
- Loesch DZ, Bui MQ, Hammersley E, Schneider A, Storey E, Stimpson P, Burgess T, Francis D, Slater H, Tassone F, Hagerman RJ, Hessler D. Psychological status in female carriers of premutation FMR1 allele showing a complex relationship with the size of CGG expansion. *Clin Genet* 2015; 87: 173-8.
- Miquel M, Toledo R, Garcia LI, Coria-Avila GA, Manzo J. Why should we keep the cerebellum in mind when thinking about addiction? *Curr Drug Abuse Rev* 2009; 2: 26-40.
- Miquel M, Vazquez-Sanroman D, Carbo-Gas M, Gil-Miravet I, Sanchis-Segura C, Carulli D, Manzo J, Coria-Avila GA. Have we been ignoring the elephant in the room? Seven arguments for considering the cerebellum as part of addiction circuitry. *Neurosci Biobehav Rev* 2016; 60: 1-11.
- Miyazaki Y, Raudenbush SW. Tests for linkage of multiple cohorts in an accelerated longitudinal design. *Psychol Methods* 2000; 5: 44-63.
- Napoli E, Song G, Wong S, Hagerman R, Giulivi C. Altered Bioenergetics in Primary Dermal Fibroblasts from Adult Carriers of the FMR1 Premutation Before the Onset of the Neurodegenerative Disease Fragile X-Associated Tremor/Ataxia Syndrome. *Cerebellum* 2016.

- O'Keefe JA, Robertson-Dick E, Dunn EJ, Li Y, Deng Y, Fiutko AN, Berry-Kravis E, Hall DA. Characterization and Early Detection of Balance Deficits in Fragile X Premutation Carriers With and Without Fragile X-Associated Tremor/Ataxia Syndrome (FXTAS). *Cerebellum* 2015; 14: 650-62.
- Oh SY, He F, Krans A, Frazer M, Taylor JP, Paulson HL, Todd PK. RAN translation at CGG repeats induces ubiquitin proteasome system impairment in models of fragile X-associated tremor ataxia syndrome. *Hum Mol Genet* 2015; 24: 4317-26.
- Polussa J, Schneider A, Hagerman R. Molecular Advances Leading to Treatment Implications for Fragile X Premutation Carriers. *Brain disorders & therapy* 2014; 3.
- Raz N, Lindenberger U, Rodrigue KM, Kennedy KM, Head D, Williamson A, Dahle C, Gerstorf D, Acker JD. Regional brain changes in aging healthy adults: general trends, individual differences and modifiers. *Cereb Cortex* 2005; 15: 1676-89.
- Rice D, Barone S, Jr. Critical periods of vulnerability for the developing nervous system: evidence from humans and animal models. *Environ Health Perspect* 2000; 108 Suppl 3: 511-33.
- Rodriguez-Revenga L, Madrigal I, Pagonabarraga J, Xuncla M, Badenas C, Kulisevsky J, Gomez B, Mila M. Penetrance of FMR1 premutation associated pathologies in fragile X syndrome families. *Eur J Hum Genet* 2009; 17: 1359-62.
- Ross-Inta C, Omanska-Klusek A, Wong S, Barrow C, Garcia-Arocena D, Iwahashi C, Berry-Kravis E, Hagerman RJ, Hagerman PJ, Giulivi C. Evidence of mitochondrial dysfunction in fragile X-associated tremor/ataxia syndrome. *Biochem J* 2010; 429: 545-52.
- Sarwar M. The septum pellucidum: normal and abnormal. *AJNR Am J Neuroradiol* 1989; 10: 989-1005.
- Scaglione C, Ginestroni A, Vella A, Dotti MT, Nave RD, Rizzo G, De Cristofaro MT, De Stefano N, Piacentini S, Martinelli P, Mascalchi M. MRI and SPECT of midbrain and striatal degeneration in fragile X-associated tremor/ataxia syndrome. *Journal of neurology* 2008; 255: 144-6.

- Scahill RI, Frost C, Jenkins R, Whitwell JL, Rossor MN, Fox NC. A longitudinal study of brain volume changes in normal aging using serial registered magnetic resonance imaging. *Arch Neurol* 2003; 60: 989-94.
- Smith SM. Fast robust automated brain extraction. *Hum Brain Mapp* 2002; 17: 143-55.
- Takahashi T, Yung AR, Yucel M, Wood SJ, Phillips LJ, Harding IH, Soulsby B, McGorry PD, Suzuki M, Velakoulis D, Pantelis C. Prevalence of large cavum septi pellucidi in ultra high-risk individuals and patients with psychotic disorders. *Schizophrenia research* 2008; 105: 236-44.
- Tassone F, Adams J, Berry-Kravis EM, Cohen SS, Brusco A, Leehey MA, Li L, Hagerman RJ, Hagerman PJ. CGG repeat length correlates with age of onset of motor signs of the fragile X-associated tremor/ataxia syndrome (FXTAS). *Am J Med Genet B Neuropsychiatr Genet* 2007; 144B: 566-9.
- Tassone F, Hagerman RJ, Taylor AK, Gane LW, Godfrey TE, Hagerman PJ. Elevated levels of *FMR1* mRNA in carrier males: a new mechanism of involvement in the fragile-X syndrome. *Am J Hum Genet* 2000; 66: 6-15.
- Tassone F, Pan R, Amiri K, Taylor AK, Hagerman PJ. A rapid polymerase chain reaction-based screening method for identification of all expanded alleles of the fragile X (*FMR1*) gene in newborn and high-risk populations. *J Mol Diagn* 2008; 10: 43-9.
- Tiemeier H, Lenroot RK, Greenstein DK, Tran L, Pierson R, Giedd JN. Cerebellum development during childhood and adolescence: a longitudinal morphometric MRI study. *Neuroimage* 2010; 49: 63-70.
- Todd PK, Oh SY, Krans A, He F, Sellier C, Frazer M, Renoux AJ, Chen KC, Scaglione KM, Basrur V, Elenitoba-Johnson K, Vonsattel JP, Louis ED, Sutton MA, Taylor JP, Mills RE, Charlet-Berguerand N, Paulson HL. CGG repeat-associated translation mediates neurodegeneration in fragile X tremor ataxia syndrome. *Neuron* 2013; 78: 440-55.

- Tustison NJ, Avants BB, Cook PA, Zheng Y, Egan A, Yushkevich PA, Gee JC. N4ITK: improved N3 bias correction. *IEEE transactions on medical imaging* 2010; 29: 1310-20.
- Walhovd KB, Westlye LT, Amlie I, Espeseth T, Reinvang I, Raz N, Agartz I, Salat DH, Greve DN, Fischl B, Dale AM, Fjell AM. Consistent neuroanatomical age-related volume differences across multiple samples. *Neurobiol Aging* 2011; 32: 916-32.
- Wang H, Das SR, Suh JW, Altinay M, Pluta J, Craige C, Avants B, Yushkevich PA, Alzheimer's Disease Neuroimaging I. A learning-based wrapper method to correct systematic errors in automatic image segmentation: consistently improved performance in hippocampus, cortex and brain segmentation. *Neuroimage* 2011; 55: 968-85.
- Wang JY, Hagerman RJ, Rivera SM. A multimodal imaging analysis of subcortical gray matter in fragile X premutation carriers. *Mov Disord* 2013a; 28: 1278-84.
- Wang JY, Hessel D, Iwahashi C, Cheung K, Schneider A, Hagerman RJ, Hagerman PJ, Rivera SM. Influence of the fragile X mental retardation (FMR1) gene on the brain and working memory in men with normal FMR1 alleles. *Neuroimage* 2013b; 65: 288-98.
- Wang JY, Hessel D, Schneider A, Tassone F, Hagerman RJ, Rivera SM. Fragile X-associated tremor/ataxia syndrome: influence of the FMR1 gene on motor fiber tracts in males with normal and premutation alleles. *JAMA neurology* 2013c; 70: 1022-9.
- Wang JY, Hessel DH, Hagerman RJ, Tassone F, Rivera SM. Age-dependent structural connectivity effects in fragile x premutation. *Arch Neurol* 2012; 69: 482-9.
- Wang JY, Ngo MM, Hessel D, Hagerman RJ, Rivera SM. Robust Machine Learning-Based Correction on Automatic Segmentation of the Cerebellum and Brainstem. *PLoS One* 2016; 11: e0156123.
- Wang SS, Kloth AD, Badura A. The cerebellum, sensitive periods, and autism. *Neuron* 2014; 83: 518-32.

A A 68-year-old control**B** A 69-year-old at stage 1**C** A 68-year-old at Stage 4**D** FXPC- vs. controls**E** Older groups



- Premutation carriers showed abnormal developmental trajectories of brain volumes.
- Premutation carriers with and without tremor/ataxia showed volume divergences.
- The volume changes showed dependencies on disease severity and CGG repeat length.
- Brain volumes are likely affected during both development and disease progression.